Mobility Tracking Based on Autoregressive Models

Zainab R. Zaidi[+] and Brian L. Mark[*]

[+] Networked Systems Group
NICTA
Eveleigh NSW 2015, Australia
email: Zainab.Zaidi@nicta.com.au

[*]Dept. of Electrical and Computer Eng.
George Mason University
4400 University Drive, MS 1G5
Fairfax, VA 22030
tel: 703-993-4069, fax: 703-993-1601
email: bmark@gmu.edu

NAPL Technical Report: Sept. 21, 2009
Number: TR-GMU-NAPL-Y09-N3
GMU Network Architecture and Performance Laboratory (NAPL)

Abstract

We propose an integrated scheme for tracking the mobility of a user based on autoregressive models that accurately capture the characteristics of realistic user movements in wireless networks. The mobility parameters are obtained from training data by computing MMSE (Minimum Mean Squared Error) estimates. Estimation of the mobility state, which consists of the position of the mobile station is accomplished via an extended Kalman filter using signal measurements from the wireless network. By combining mobility parameter and state estimation in an integrated framework, we obtain an efficient and accurate real-time mobility tracking scheme that can be applied in a variety of wireless networking applications. We consider two variants of an autoregressive mobility model in our study and validate the proposed mobility tracking scheme using mobile trajectories collected from drive test data. Our simulation results validate the accuracy of the proposed tracking scheme even when only a small number of data samples are available for initial training.

Index Terms

Mobility model, Geolocation, Autoregressive model, Kalman filter, Yule-Walker equations

I. Introduction

User mobility is a fundamental characteristic of wireless mobile networks that profoundly impacts network performance. To perform optimally, a wireless network should be designed to take into account the mobility of the user. In this regard, two issues of fundamental importance are: 1) the development of suitable models of user mobility to drive realistic simulations of wireless networks and 2) efficient real-time tracking of user mobility to enable seamless connectivity and quality-of-service in a wireless network. The two issues are closely interrelated, since accurate real-time tracking of user mobility must be based on an appropriate mobility model that can be used to anticipate the future mobility state of the user. Conversely, in order to generate realistic mobility patterns for the purpose of simulating a wireless network, actual mobile trajectories from live networks should be fit to a model that can capture the salient characteristics of user mobility. Furthermore, accurate mobility tracking requires that the parameters of the mobility model be matched as closely as possible to the available data.

Some of the more prominent mobility models (cf. [1], [2]) that have been proposed in the literature include random walk models [3], the random waypoint model [4], Brownian motion models [5], Gauss-Markov models [6], and Markov chain models [7]. Such models have the important feature of simplicity, making them amenable for use in simulation and in some cases analytical modeling of wireless network behavior. However, more recent studies have shown that many of them do not accurately represent actual user trajectories in real wireless networks [2], [8]–[10]. Consequently, such models may provide misleading characterizations of network performance.

Another class of mobility models employs additional information to improve the accuracy of mobility representation. The additional information may consists of a terrain map or street layout [11], [12], traffic conditions [13], hotspots or regions of interest [14], [15], obstacle's shapes and locations [16], behavioral rules to represent typical human responses [17], etc. However, the applicability of such models may be limited since the parameters for one scenario may not be

usable in other environments. Since the modeling assumptions are not validated with real data and compared with other models, the accuracy achieved by this class of models is difficult to evaluate quantitatively. Moreover, such models are not sufficiently rich to enable accurate and precise real-time mobility tracking.

A linear system model of mobility has been applied to real-time mobility tracking via various state estimation methods, such as Kalman filters [18]–[20], sequential Monte Carlo filtering [21], particle filters [22], and predictive methods [6]. In this model, the mobility state consists of position, velocity, and acceleration. The linear system model is capable of capturing realistic user mobility patterns, but specification of an optimal set of model parameters is not straightforward. Mobility tracking schemes derived from the linear system model are accurate as long as the model parameters match the mobility characteristics of the user. However, accuracy of the model parameters is difficult to achieve in practice.

In this paper, we study two models of mobility based on autoregressive (AR) models, which are amenable to parameter estimation. The first is a sampled version of an underlying continuous-time, first-order AR model. We refer to this model as the *AR-1 model*. In the AR-1 model, the mobility state consists of the position, velocity, and acceleration of the mobile at a given time instant. The AR-1 model was first introduced in [23]. A more comprehensive study, including comparative analysis with other mobility models, convergence issues, effects of training data, and efficacy of AR-1 model in representing broader range of trajectories, is given in the present paper.

The AR-1 model is a variant of the linear system model with the key feature that it is amenable to MMSE (Minimum Mean Squared Error) estimation of the model parameters. Optimal parameter estimation is generally not possible with the linear system model of mobility used in [18], [19], [21]. The AR-1 model is sufficiently simple to enable real-time mobility tracking, but general enough to accurately capture the characteristics of realistic mobility patterns in wireless networks by means of optimal estimation of model parameters.

The second AR-based model, which we call the *Position-AR* model, is a discrete-time model

in which the mobility state consists of the mobile's position at consecutive time points. In the Position-AR model, velocity and acceleration are represented as finite differences of position coordinates. As we shall discuss in this paper, parameter and state estimation algorithms for the Position-AR model have smaller computational complexity than the AR-1 model. Our numerical results show that the Position-AR model requires less training data for parameter estimation.

Based on the AR-1 and Position-AR mobility models, we develop a mobility tracking scheme that integrates MMSE estimation for the unknown model parameters with mobility state estimation using Kalman filtering. The mobility tracking scheme can adapt to changes in the mobility characteristics over time, since the model parameters are continuously re-estimated using new observation data. Our numerical results using drive test data show that the AR-1 and Position-AR models can accurately capture realistic mobility patterns. Without a systematic approach to parameter estimation, the existing mobility models cannot make a similar claim.

The main contribution of this paper is a mobility tracking scheme that simultaneously estimates both the mobility state of a mobile user and the unknown parameters of the mobility model, in this case the AR-1 and Position-AR models. As discussed earlier, other models of mobility proposed in the literature are not amenable to parameter estimation and hence cannot be used in practice to accurately model real mobility traces. Our numerical results show that the proposed mobility tracking algorithm, based on either the AR-1 or the Position-AR model, converges quickly and yields accurate performance when a sufficient amount of training data is provided for initialization. The algorithm is computationally feasible for real-time tracking applications, as it requires a small number of Kalman filtering and MMSE estimation steps to be performed at each discrete-time instant. Comparison between the AR-1 and Position-AR models show that the Position-AR model yields a mobility tracking scheme that has smaller computational complexity and is more robust to variations in operational settings such as the number of available training samples and the distance between mobile nodes and base stations.

The remainder of the paper is organized as follows. Section II describes the AR-1 and Position-AR models. Procedures for optimal estimation of the model parameters in the MMSE sense are

developed in Section III. The parameter estimation procedure is one component of an integrated scheme for real-time mobility tracking. Section IV discusses the second component of mobility state estimation via Kalman filtering using various types of signal measurements from the wireless network as observation data. Section V presents a detailed validation of the AR-1 and Position-AR mobility models and their associated mobility tracking schemes using drive test data collected from the field. Finally, Section VI concludes the paper.

II. Autoregressive Mobility Models

Autoregressive models have been used to model mobility in wireless networks, such as, the Gauss-Markov model [6], the position and velocity model [20], etc. The Global Positioning System (GPS) uses a variety of autoregressive-based models, including one called the PVA (position, velocity, and acceleration) model [24]. However, the issue of how to select the appropriate model parameters to represent realistic mobility patterns has not been treated for these models, nor in the available literature on mobility modeling for wireless networks (cf. [1], [2]). In this section, we propose two variants of autoregressive models to represent user mobility in a wireless network. Parameter estimation for these models is discussed in Section III.

A. AR-1 Model

The AR-1 model is a discrete-time model of mobility such that the mobility state at time index n is given by $\boldsymbol{s}_{1,n} = [x_n, \dot{x}_n, \ddot{x}_n, y_n, \dot{y}_n, \ddot{y}_n]'$, where x_n and y_n denote the x and y coordinates, $\dot{x}_n$ and $\dot{y}_n$ represent the speed, and $\ddot{x}_n$ and $\ddot{y}_n$ represent the acceleration of a mobile unit at discrete time instant n in two-dimensional space. The notation $'$ indicates the matrix transpose operator. If mobility state information is needed in three dimensions, the $\boldsymbol{s}_{1,n}$ vector can be augmented by $[z_n, \dot{z}_n, \ddot{z}_n]'$, where the vector elements represent position, velocity, and acceleration in the z-dimension. We characterize the dynamics of the mobility state process $\{\boldsymbol{s}_{1,n}\}$ by a first-order autoregressive (AR-1) model given as follows:

$$\boldsymbol{s}_{1,n+1} = A_1 \boldsymbol{s}_{1,n} + \boldsymbol{w}_{1,n}, \tag{1}$$

where A_1 is a 6×6 transformation matrix and $\boldsymbol{w}_{1,n}$ is a zero mean, white Gaussian vector process with covariance matrix Q_1. The matrices A_1 and Q_1 can be estimated from the trajectory data using Yule-Walker equations as will be discussed in Section III.

B. Position-AR Model

Position-AR is also a discrete-time model of mobility but the mobility state at time index n is given by $\boldsymbol{s}_{2,n} = [x_n, x_{n-1}, x_{n-2}, y_n, y_{n-1}, y_{n-2}]'$, where x_n and y_n denote the x and y coordinates of a mobile unit at discrete time instant n. The dynamics equation of the Position-AR model is given by,

$$\boldsymbol{s}_{2,n+1} = A_2\boldsymbol{s}_{2,n} + \boldsymbol{w}_{2,n}, \tag{2}$$

where A_2 is a 6×6 transformation matrix and $\boldsymbol{w}_{2,n}$ is a zero mean, white Gaussian vector process with covariance matrix Q_2.

The elements of the matrix A_2 specify the relationships among position, velocity, and acceleration from time nT to time $(n+1)T$, where T is the time interval between successive samples. In the x-direction, the following holds:

$$x_{n+1} \;=\; x_n + T\dot{x}_n + \frac{T^2}{2}\ddot{x}_n. \tag{3}$$

Using finite differences, $\dot{x}_n$ and $\ddot{x}_n$ can be approximated as follows:

$$\dot{x}_n \;=\; \frac{x_n - x_{n-1}}{T}, \tag{4}$$

$$\ddot{x}_n \;=\; \frac{\dot{x}_n - \dot{x}_{n-1}}{T} = \frac{x_n - 2x_{n-1} + x_{n-2}}{T^2}. \tag{5}$$

Substituting (4) and (5) into (3), we obtain

$$x_{n+1} = 2.5x_n - 2x_{n-1} + 0.5x_{n-2}. \tag{6}$$

A set of equations analogous to (6) can be written to characterize the system dynamics in the y-direction. Hence, the matrix A_2 is given as

$$A_2 = \begin{bmatrix} A_x & 0_{3\times3} \\ 0_{3\times3} & A_y \end{bmatrix}, \tag{7}$$

where $0_{3\times3}$ is the 3×3 matrix of all zeros and

$$A_x = A_y = \begin{bmatrix} 2.5 & -2 & 0.5 \\ 1 & 0 & 0 \\ 0 & 1 & 0 \end{bmatrix}.$$

Since A_2 is a constant matrix, as opposed to the unknown A_1 matrix of the AR-1 model, the estimation of the covariance matrix Q_2 completely specifies the Position-AR mobility model.

C. Comparison with other mobility models

Comparing the state equations (1) with that of the linear system model discussed in [18], the linear system model includes an extra term $B\boldsymbol{u}_n$, where B is a 6×2 matrix and $\boldsymbol{u}_n$ is a vector of two independent semi-Markov discrete command processes that drive the acceleration of the model in the two-dimensional plane. In the linear system model of [18] and [19], the matrices A and B are specified in terms of the sampling interval T and a parameter α. The command process $\boldsymbol{u}_n$ is specified by a set of discrete command levels, a transition probability matrix, and probability distributions for the durations in each command level. An outstanding issue for the linear system model is the question of how to specify an appropriate set of parameters.

The Position-AR and AR-1 models are more general than the Gauss-Markov model proposed in [6]. In the Gauss-Markov model of [6], the mobility state consists of position, velocity, and direction, but does not explicitly represent acceleration. A key feature of the Gauss-Markov model with respect to simpler mobility models is that the correlation between successive velocity states is explicitly modeled via a gain parameter α. A similar model was used in [20] as the basis for a location tracking scheme. The AR-1 model captures not only the correlation between velocity states, but also the correlation between acceleration states. Similarly, the Position-AR model incorporates the last three successive position coordinates in order to represent the current position so that the effect of velocity, as well as, acceleration is incorporated into the model.

A significant benefit of the Position-AR and AR-1 models is that they can be used to provide predictive mobility information. If the state information or estimate $\hat{\boldsymbol{s}}_n$ at a given time n is

available, it is possible to predict the mobility state at any time $n+m$ in the future. From the theory of autoregressive processes (cf. [25]), the optimal predicted state $\boldsymbol{s}^*_{n+m|n}$ of a mobile node in the minimum mean-squared error (MMSE) sense, given the state estimate $\hat{\boldsymbol{s}}_n$ at time n, can be obtained as

$$\boldsymbol{s}^*_{n+m|n} = E[\boldsymbol{s}_{n+m}|\hat{\boldsymbol{s}}_n] = A^m \hat{\boldsymbol{s}}_n, \tag{8}$$

where A could be A_1 or A_2 and the mobility state $\hat{\boldsymbol{s}}_n$ could be $\hat{\boldsymbol{s}}_{1,n}$ or $\hat{\boldsymbol{s}}_{2,n}$, depending on which of the two mobility models is used. The associated covariance matrix for the predicted mobility state at time $n+m$, denoted $M^*_{n+m|n} = \text{Cov}[\boldsymbol{s}^*_{n+m}|\hat{\boldsymbol{s}}_n]$, is given by

$$M^*_{n+m|n} = A^m M_n A'^m + \sum_{l=0}^{m-1} A^{m-1-l} Q A'^{m-1-l}, \tag{9}$$

where $M_n = \text{Cov}[\hat{\boldsymbol{s}}_n]$ and Q could be Q_1 or Q_2. Knowledge of the predicted mobility state can be used to devise anticipatory resource allocation schemes for wireless networks. For example, the predicted mobility state could be incorporated into IP mobility management protocols [26], [27] to provide more seamless handoffs (cf. [28]). Existing geolocation systems generally track only the current location of the mobile and do not provide this predictive capability.

According to Bettstetter's nomenclature for mobility models [1], the AR-1 and Position-AR models may be classified as *microscopic* mobility models. A microscopic model describes the movement, i.e., position, velocity etc., of an individual vehicle or person as opposed to a model describing group behavior such as the fluid flow model, group mobility model [29], gravity models [30], map or activity based models [31], [32], etc. Such composite mobility models are constructed from microscopic models (cf. [2]). Thus, the AR-1 and Position-AR models could be used as building blocks to develop more sophisticated models of mobility for various network scenarios.

III. Mobility Parameter Estimation

In this section, we discuss algorithms for obtaining the MMSE (Minimum Mean Squared Error) estimates of the parameters for the AR-1 and Position-AR models based on training data.

Using the parameter estimates, the AR-1 and Position-AR models can be used to generate realistic mobility patterns for simulation purposes, given a suitable set of training samples obtained from the field.

A. AR-1 Parameter Estimation

Using the Yule-Walker equations [25], an optimal estimate of A_1 in the MMSE sense, denoted $\hat{A}_1^{(n)}$, where n specifies the amount of training data available, can be found from the mobility state data $\boldsymbol{s}_{1,1}, \cdots, \boldsymbol{s}_{1,n}$ as follows:

$$\hat{A}_1^{(n)} = R_{\boldsymbol{s}}^{(n)}(1) R_{\boldsymbol{s}}^{(n)}(0)^{-1}, \tag{10}$$

where

$$R_{\boldsymbol{s}}^{(n)}(1) = \frac{1}{n-2} \sum_{i=1}^{n-1} \boldsymbol{s}_{1,i} \boldsymbol{s}'_{1,i+1}, \tag{11}$$

$$R_{\boldsymbol{s}}^{(n)}(0) = \frac{1}{n-1} \sum_{i=1}^{n} \boldsymbol{s}_{1,i} \boldsymbol{s}'_{1,i}. \tag{12}$$

The estimator $\hat{A}_1^{(n)}$ is a Minimum Mean Squared Error (MMSE) estimator and can be directly derived from the orthogonality principle. The noise covariance matrix $\hat{Q}_1^{(n)}$ is estimated using the residual estimation error, $\boldsymbol{e}_i \triangleq \boldsymbol{s}_{1,i} - \hat{A}_1^{(i)} \boldsymbol{s}_{1,i-1}$, as follows:

$$\hat{Q}_1^{(n)} = \frac{1}{n-1} \sum_{i=1}^{n} \boldsymbol{e}_i \boldsymbol{e}'_i. \tag{13}$$

An extended Kalman filter, described in Section IV-B, is used to generate the mobility state estimates $\hat{\boldsymbol{s}}_{1,n}$ from the wireless measurements $\boldsymbol{o}_n$ at time n. The state estimates $\hat{\boldsymbol{s}}_{1,n}$ are used to re-estimate the model parameters at time n. The recursive model parameter estimator is given below.

Recursive parameter estimation (time $n = 1, 2, \cdots$):

1) $R_{\boldsymbol{s}}^{(n)}(0) = \frac{1}{n-1} \left((n-2) R_{\boldsymbol{s}}^{(n-1)}(0) + \hat{\boldsymbol{s}}_{1,n} \hat{\boldsymbol{s}}'_{1,n} \right)$
2) $R_{\boldsymbol{s}}^{(n)}(1) = \frac{1}{n-2} \left((n-3) R_{\boldsymbol{s}}^{(n-1)}(1) + \hat{\boldsymbol{s}}_{1,n-1} \hat{\boldsymbol{s}}'_{1,n} \right)$
3) $\hat{A}_1^{(n)} = R_{\boldsymbol{s}}^{(n)}(1) R_{\boldsymbol{s}}^{(n)}(0)^{-1}$
4) $\boldsymbol{e}_n = \hat{\boldsymbol{s}}_{1,n} - \hat{A}_1^{(n)} \hat{\boldsymbol{s}}_{1,n-1}$
5) $\hat{Q}_1^{(n)} = \frac{1}{n-1} \left((n-2) \hat{Q}_1^{(n-1)} + \boldsymbol{e}_n \boldsymbol{e}'_n \right)$

Here we have assumed that a sufficient amount of training data is available to initialize $R_{\boldsymbol{s}}^{(0)}(0)$ and $R_{\boldsymbol{s}}^{(0)}(1)$. In practice, some information may be available to initialize or train the mobility estimator. For example, our mobility tracking method may be used alongside GPS to cover the holes in satellite coverage; in this case, the GPS data may provide training samples for the mobility estimator. We can also use relationships between position, velocity, and acceleration as shown in (3) to initialize $\hat{A}_1^{(0)}$. Initialization of parameter estimation without any training data is also discussed in Section V.

B. Position-AR Parameter Estimation

As discussed above, the Position-AR mobility model is completely specified by the covariance matrix Q_2 of the noise. The MMSE estimators for Q_2, denoted by $\hat{Q}_2$, can be obtained from (13) when residual error is defined as $\boldsymbol{e}_i \triangleq \boldsymbol{s}_{2,i} - A_2\boldsymbol{s}_{2,i-1}$. Similarly the recursive estimation for noise covariance matrix designed for the AR-1 model can be used with the Position-AR covariance matrix when the residual errors are calculated with A_2 and $\hat{\boldsymbol{s}}_{2,n}$ and the initial estimate $\hat{Q}_2^{(0)}$ is determined from a set of training samples as discussed above.

IV. Mobility Tracking Scheme

Our proposed mobility tracking scheme consists of the parameter estimation algorithms discussed in Section III combined with mobility state estimation, which we shall discuss in this section. The integrated mobility tracking scheme is shown in Fig. 1. In Fig. 1, the state estimate $\hat{\boldsymbol{s}}_n$ could be $\hat{\boldsymbol{s}}_{1,n}$ or $\hat{\boldsymbol{s}}_{2,n}$ depending on whether the underlying mobility model is AR-1 or Position-AR. Similarly, $\hat{Q}$ could be $\hat{Q}_1$ or $\hat{Q}_2$ and $\hat{A}$ could be $\hat{A}_1$ or A_2, since the transformation matrix is fixed in the case of the Position-AR model. Although not explicitly shown in Fig. 1, the Kalman filter includes a pre-filter (cf. [33]) to reduce the effects of measurement noise.

A. Observation Data in Wireless Networks

To perform mobility state estimation, we assume that either received signal strength indicators (RSSI) or time of arrival (TOA) measurements from at least three base stations are available. We remark that the angle of arrival (AOA) of the mobile's signal at multiple base stations is often

used for location tracking [34]–[36]. The AOA is typically estimated using antenna arrays at the base station. However, AOA information is not suitable for use in conjunction with an extended Kalman filter, since the AOA measurements are non-continuous functions of mobility state that are generally not differentiable. Another measurement used to locate the mobile callers is the time difference of arrival (TDOA) of the signals from two base stations [34], [37], [38]. However, calculation of the TDOA requires time synchronization of the base stations. Moreover, when three base stations are used to provide TDOA measurements, there is often more than one localization solution and, as observed in [34], [39], there is no way to determine the correct solution without the help of additional information, e.g., additional TOA measurements as suggested by [39].

1) Pilot Signal Strengths: In a wireless cellular network, the distance between the mobile and a reachable base station can be inferred from the RSSI (Received Signal Strength Indication) or pilot signal strength from the base station. Pilot signal strengths are more readily available in wireless networks than TOA, TDOA, and AOA signals, which require specialized infrastructure to collect useful data. On the other hand, the effectiveness of using RSSI to infer distance information depends on the accuracy of the signal propagation model. The lognormal shadow fading model has proved to be accurate for a large class of urban and suburban environments [40]. According to this model, the RSSI, in units of dB, received at the mobile unit from base station i, located at position (a_i, b_i) at time n is given as follows [41]:

$$p_{n,i} = \kappa_i - 10\gamma \log(d_{n,i}) + \psi_{n,i}, \tag{14}$$

where κ_i is a constant determined by the transmitted power, antenna height, wavelength, and gain of the base station i, γ is a slope index (typically γ is between $2-5$), $\psi_{n,i}$ is a zero mean, stationary Gaussian process with standard deviation σ_ψ typically from $4-8$ dB, and $d_{n,i}$ is the distance between the mobile node and base station i:

$$d_{n,i} = \sqrt{(x_n - a_i)^2 + (y_n - b_i)^2}. \tag{15}$$

The noise process $\psi_{n,i}$ models shadowing or slow fading, while fast fading is neglected in (14), under the assumption that it is attenuated sufficiently via low pass filtering (cf. [18], [42]).

Distance measurements to three independent base stations are sufficient to locate the mobile unit in the two-dimensional plane. For mobility estimation based on RSSI information, we construct an observation vector consisting of the three largest RSSI measurements, denoted by $p_{n,1}$, $p_{n,2}$, $p_{n,3}$, as follows:

$$\boldsymbol{o}_n = (p_{n,1}, p_{n,2}, p_{n,3})' = h(\boldsymbol{s}_n) + \boldsymbol{\psi}_n, \tag{16}$$

where $\boldsymbol{s}_n$ could be mobility state defined for either the AR-1 or the Position-AR model, $\boldsymbol{\psi}_n = (\psi_{n,1}, \psi_{n,2}, \psi_{n,3})'$, and

$$h(\boldsymbol{s}_n) = \boldsymbol{\kappa} - 10\gamma \log(\boldsymbol{d}_n), \tag{17}$$

where $\boldsymbol{\kappa} = (\kappa_1, \kappa_2, \kappa_3)'$ and $\boldsymbol{d}_n = (d_{n,1}, d_{n,2}, d_{n,3})'$. The covariance matrix of $\boldsymbol{\psi}_n$ is given by $R_\psi = \sigma_\psi^2 I_3$ where I_3 is the 3×3 identity matrix.

2) Time of Arrival (TOA): Time-based methods of geolocation using TOA and TDOA measurements rely on accurate estimates of the time of arrival of the signals received at several base stations from the mobile station or at the mobile station from several base stations [34], [37]. Several approaches have been developed for estimation of these parameters from received signals such as code tracking and acquisition in spread spectrum systems using delay-locked loop (DLL) or tau-dither loop as described in [34]. In the presence of measurement noise, the time delay estimate of the signal $\tau_{n,i}$, from base station i measured at the mobile station, at time instant n using DLL is given by

$$\tau_{n,i} = d_{n,i}/c + \psi_{n,i}, \tag{18}$$

where $d_{n,i}$ is given in (15), c is the speed of light. In contrast to the RSSI model (14), here $\psi_{n,i}$ represents zero mean, white Gaussian noise, with a typical standard deviation of $\sigma_\psi = 1$ μs [43].

As in the case of pilot signal strengths, three TOA measurements to neighboring base stations are sufficient for mobility state estimation. The observation vector for TOA-based mobility estimation consists of the three TOA measurements, denoted by $\boldsymbol{o}_n = (\tau_{n,1},\ \tau_{n,2},\ \tau_{n,3})'$. In

this case, the observation equation is given by

$$\boldsymbol{o}_n = h(\boldsymbol{s}_n) + \boldsymbol{\psi}_n, \tag{19}$$

where $\boldsymbol{s}_n$ could be the mobility state defined for either the AR-1 or the Position-AR model, $\boldsymbol{\psi}_n = (\psi_{n,1}, \psi_{n,2}, \psi_{n,3})'$, and

$$h(\boldsymbol{s}_n) = \boldsymbol{d}_n/c, \tag{20}$$

where $\boldsymbol{d}_n = (d_{n,1}, d_{n,2}, d_{n,3})'$. As in (16), the covariance matrix of the measurement noise $\boldsymbol{\psi}$ is denoted by $R_\psi = \sigma_\psi^2 I_3$.

B. Application of Kalman filter

To apply the extended Kalman filter for state estimation, the observation equation given in (16) and (19) can linearized as follows:

$$\boldsymbol{o}_n = h(\boldsymbol{s}_n^*) + H_n \Delta \boldsymbol{s}_n + \boldsymbol{\psi}_n, \tag{21}$$

where $\boldsymbol{s}_n^*$ is the nominal or reference vector and $\Delta \boldsymbol{s}_n = \boldsymbol{s}_n - \boldsymbol{s}_n^*$ is the difference between the true and nominal state vectors. In the extended Kalman filter (cf. [24]), the nominal vector is obtained from the estimated state trajectory $\hat{\boldsymbol{s}}_n$, i.e., $\boldsymbol{s}_n^* = \hat{\boldsymbol{s}}_n$. The matrix H_n is given by

$$H_n = \frac{\partial h}{\partial \boldsymbol{s}} \mid_{\boldsymbol{s}=\hat{\boldsymbol{s}}_n} \tag{22}$$

Expressions for the matrix H_n for both RSSI and TOA measurements are given in the Appendix.

Let $\boldsymbol{o}_i^j = (\boldsymbol{o}_i, \cdots, \boldsymbol{o}_j)$ denote the set of observations from time i to time j for $j > i$. The Kalman filter estimates are denoted as follows:

$$\hat{\boldsymbol{s}}_{n|n} = E[\boldsymbol{s}_n | \boldsymbol{o}_1^n] \text{ and } \hat{\boldsymbol{s}}_{n|n-1} = E[\boldsymbol{s}_n | \boldsymbol{o}_1^{n-1}].$$

The covariance matrices corresponding to these estimates are denoted by

$$M_{n|n} = \text{Cov}[\boldsymbol{s}_n | \boldsymbol{o}_1^n] \text{ and } M_{n+1|n} = \text{Cov}[\boldsymbol{s}_{n+1} | \boldsymbol{o}_1^n],$$

respectively. The Kalman filter procedure for state estimation is then given as follows:

Mobility state estimation (time $n = 2, 3, \cdots$):

1) $H_n = \frac{\partial h}{\partial \boldsymbol{s}} \mid_{\boldsymbol{s}=\hat{\boldsymbol{s}}_n}$

2) $K_n = M_{n|n-1} H_n' (H_n M_{n|n-1} H_n' + R_\psi)^{-1}$

3) $\hat{\boldsymbol{s}}_{n|n} = \hat{\boldsymbol{s}}_{n|n-1} + K_n(\boldsymbol{o}_n - h(\hat{\boldsymbol{s}}_{n|n-1}))$ [Correction step]

4) $M_{n|n} = (I - K_n H_n) M_{n|n-1} (I - K_n H_n)' - K_n R_\psi K_n'$

5) $\hat{\boldsymbol{s}}_{n+1|n} = \hat{A}^{(n)} \hat{\boldsymbol{s}}_{n|n}$ [Prediction step]

6) $M_{n+1|n} = \hat{A}^{(n)} M_{n|n} \hat{A}^{(n)\prime} + \hat{Q}^{(n)}$

In the above procedure, the matrices $\hat{A}^{(n)}$ and $\hat{Q}^{(n)}$ correspond to the nth estimate of the transformation and covariance matrices of both mobility models, as indicated in Figure 1. For the Position-AR model, the matrix $\hat{A}^{(n)}$ is replaced by the constant matrix in (7). The matrix K_n is referred to as the Kalman gain matrix. The mobility state estimate at time n is then defined by $\hat{\boldsymbol{s}}_n \triangleq \hat{\boldsymbol{s}}_{n|n}$. The initialization of the Kalman filter is specified by

$$\hat{\boldsymbol{s}}_{1|0} = E[\boldsymbol{s}_1] \text{ and } M_{1|0} = \mathrm{Cov}[\boldsymbol{s}_1].$$

In practice, we set the initial parameters for both mobility models as follows:

$$\hat{\boldsymbol{s}}_{1|0} = (\hat{x}_1, 0, 0, \hat{y}_1, 0, 0)' \text{ and } M_{1|0} = I_6,$$

where $(\hat{x}_1, \hat{y}_1)$ is the best available estimate of the initial position of the mobile unit. In practice, some information may be available to initialize the mobility estimator. For example, knowledge of the approximate location of the mobile user, e.g., the median coordinate values of the cell sector in which the user resides, could be used to initialize the mobility state vector. As another example, our mobility tracking method may be used alongside GPS to cover the holes in satellite coverage; in this case, the GPS data may provide initial state vector along with training data for model parameter estimation.

C. Relationship to EM algorithm and convergence

The mobility tracking scheme of Fig. 1 can be viewed as a realization of the EM (Expectation-Maximization) algorithm (cf. [44]). The E-step of the EM algorithm corresponds to the estimation of hidden data by observations (or incomplete data) by finding (cf. [44])

$$\hat{\boldsymbol{s}}_n = E[\boldsymbol{s}_n | \boldsymbol{o}_n, \theta_{n-1}], \tag{23}$$

where θ_n denotes the nth estimates of unknown model parameters, e.g., $\hat{A}^{(n)}$ and $\hat{Q}^{(n)}$ for the AR-1 model and $\hat{Q}^{(n)}$ for the Position-AR mobility model. Equation (23) holds for the Kalman filter [24], and holds approximately for the extended Kalman filter, provided the difference between the true and nominal trajectory, i.e., $\Delta \boldsymbol{s}_n = \boldsymbol{s}_n - \boldsymbol{s}_n^* = \boldsymbol{s}_n - \hat{\boldsymbol{s}}_{n|n-1}$, remains small.

The M-step of the EM algorithm [44] relates to parameter estimation. Let $\hat{\theta}_n$ denote the nth estimate of an unknown parameter θ. In the M-step, $\hat{\theta}_n$ is computed such that it maximizes the expected likelihood of unknown data, given the observations and current parameter estimates [44], i.e.,

$$\hat{\theta}_n = \arg\max_{\theta} E[\log p(\boldsymbol{s}_1, \cdots, \boldsymbol{s}_n|\theta)|\boldsymbol{o}_n, \hat{\theta}_{n-1}], \tag{24}$$

where $\boldsymbol{o}_n$ denotes the nth observation and $\boldsymbol{s}_1$, $\cdots$, $\boldsymbol{s}_n$ denote the system states from time 1 to n. Using the first-order autoregressive property of the AR-1 and Position-AR mobility models and the assumption that (23) holds, the M-step in (24) can be written as:

$$\begin{aligned}\hat{\theta}_n = \arg\max_{\theta} \Bigg[& -\frac{n}{2}\log\left((2\pi)^6|Q|\right) \\ & - \frac{1}{2}\sum_{i=1}^{n}(\hat{\boldsymbol{s}}_i - A\hat{\boldsymbol{s}}_{i-1})Q^{-1}(\hat{\boldsymbol{s}}_i - A\hat{\boldsymbol{s}}_{i-1})'\Bigg]\end{aligned} \tag{25}$$

Carrying out the maximization in (25) yields an estimate for A of the form (10) and an estimate for Q of the form (13).

As long as $\Delta \boldsymbol{s}_n$ is kept small, the convergence properties that derived for the EM algorithm carry over to the proposed mobility tracking scheme. In particular, it can be shown that under certain conditions, the estimates for A and Q will converge to a stationary point of the likelihood function, which could be a global or local maximum or a saddle point (cf. [45, Section 2.1]). Convergence of the mobility state estimator depends on issues related to extended Kalman filters. An important factor to reduce numerical roundoff errors is to initialize the filter with proper initial estimates (cf. [24, pp. 260-264, 346]). Convergence of Kalman filters is also dependent on the observability of the system [24]. In [33], the observability issue was investigated in the case of the linear dynamic system model. Similar analysis for the AR-1 and Position-AR models shows

that the extended Kalman filter is observable under fairly general conditions when three or more observations are used.

V. Numerical Results

In this section, we present some representative numerical results to validate the effectiveness of the AR-1 and Position-AR models and the associated mobility tracking schemes. We apply both models to mobility patterns obtained from drive tests, as well as those generated by alternative mobility models such as the random waypoint and linear system models and compare the respective estimation results under various operating conditions.

A. Data Collection

The data of interest, collected from a drive test data, consisted of latitude and longitude values of the mobile user at pre-defined measurement time intervals. The drive test was converted from latitude/longitude (Lat/Long) coordinates, in decimal format, to two-dimensional Cartesian coordinates (x, y) as follows:

$$x = C\frac{\pi \cos(\text{Lat}_0)}{180}(\text{Long}_0 - \text{Long}) \tag{26}$$

$$y = C\frac{\pi}{180}(\text{Lat} - \text{Lat}_0) \tag{27}$$

where $C = 6378137$ and $(\text{Lat}_0, \text{Long}_0)$ correspond to the latitude and longitude, in decimal format, of the origin $(0, 0)$ of the local Cartesian coordinate system. To facilitate the performance evaluation of the proposed mobility tracking algorithms, we generated RSSI and TOA measurements using (14) and (18), respectively, with fixed parameter values. As such, our results do not take into account the effects of measurement or propagation modeling error in the field. Our intent was to focus on validating the effectiveness of the AR-1 and Position-AR models in characterizing user mobility.

B. Validation of Mobility Model

We collected three sets of drive test data containing more than 1200 sample points each. One set of data was collected from a suburban area while another set was obtained from a downtown

city environment with an orthogonal street layout. The third drive test was carried out by a walking subject in the Fairfax campus of George Mason University (GMU). The drive test data consisted of a sequence of (x, y)-coordinates characterizing the trajectory of the mobile user. For each data set, we construct a corresponding mobility state sequence $\{\boldsymbol{s}_1, \cdots \boldsymbol{s}_{N_T}\}$ for both models, where N_T denotes the total number of data points.

To validate the accuracy of the mobility model, we use the multiple coefficient of determination, denoted by R^2 (cf. [46], [47]). For each of the mobility state sequences, we use the first N mobility states as training samples to obtain estimates $\hat{A}_1$ and $\hat{Q}_1$ for the AR-1 model and $\hat{Q}_2$ for the Position-AR model, as discussed in Section III. The remaining mobility states, $\boldsymbol{s}_{N+1}, \cdots, \boldsymbol{s}_{N_T}$, are then used to compute the R^2 metric as follows:

$$R^2 = 1 - \frac{\sum_{i=N+1}^{N_T} |\boldsymbol{s}_i - A\boldsymbol{s}_{i-1}|^2}{\sum_{i=N+1}^{N_T} |\boldsymbol{s}_i - \bar{\boldsymbol{s}}|^2}, \tag{28}$$

where $\boldsymbol{s}_i$ is the ith mobility state for either model and

$$\bar{\boldsymbol{s}} = \frac{1}{N_T - N} \sum_{i=N+1}^{N_T} \boldsymbol{s}_i$$

is the sample average of the mobility state sequence after the first N states. The value of R^2 always lies in the interval $[0, 1]$. A value of R^2 close to 1 indicates a strong model fit. Table I shows the R^2 values for the three data sets for the AR-1 and Position-AR models. The results demonstrate that statistically accurate mobility characterization in terms of the AR-1 and Position-AR models can be obtained.

The sampling interval of one second is relatively short compared to the dynamics of our drive test trajectories. Hence, each of the sampled trajectories closely follows the corresponding actual trajectory even though the mobility trace may appear to be highly nonlinear. Consequently, both the AR-1 and Position-AR mobility estimators perform well with respect to the R^2 metric, as shown in Table I. Note that slightly lower R^2 value is obtained for the walking scenario compared to the suburban scenario. Similarly, compared to the suburban and walking scenarios, five times the number of training samples is needed in the urban scenario to achieve an R^2 value of 0.95 or higher for both estimators. These results can be explained in terms of Fig. 4, which

visually shows that both the walking and urban trajectories contain more turns and bends than the suburban trajectory.

The noise terms in the AR-1 and Position-AR models are assumed to be zero mean white Gaussian noise processes. To check the validity of this assumption, we use residual error analysis (cf. [47]). The residual error for a data point s_i is defined as $e_i = s_i - \hat{s}_i$. The plots in Fig. 2 show that the residual errors in the x and y dimensions seem to be independent of the data points. These plots were generated for the Position-AR model using the suburban trajectory data with model parameter estimation as described in Section III. Other data sets also show similar characteristics. Fig. 3 shows two Q-Q plots (cf. [47]) for residual errors for the Position-AR model in the x and y dimensions. The close straight-line fit observed in both plots confirms the validity of the assumption that the residual errors or model noise can be modeled accurately by white Gaussian processes. Similar graphs for the AR-1 model are presented in [23].

C. Validation of Mobility Estimation Scheme

We simulated test scenarios to validate the effectiveness of the mobility estimation scheme based on the AR-1 and Position-AR models (cf. Section IV). We assume that the service area is subdivided into a rectangular grid with square cells. Each cell contains one base station located in the center of the cell. In our simulation experiments, a mobile user moving along a drive test trajectory receives signals (either RSSI or TOA) from the base stations and employs the integrated mobility estimator to determine the mobility state as well as the parameters of the underlying AR-1 or Position-AR model. A training set consisting of the first few data points in the actual mobility state sequence is used to obtain the initial estimates $\hat{A}_1$ and $\hat{Q}_1$ of the AR-1 model and $\hat{Q}_2$ of the Position-AR model.

The RSSI measurements are generated using (14) with the parameter κ assumed to be zero for all base stations and γ set to 5 for all scenarios. Typical values for the shadowing noise standard deviation, i.e., σ_ψ, range from $4-8$ dB [41]. The shadowing standard deviation is taken as 8 dB. The TOA measurements are generating using (18). The error noise in the TOA measurements

is assumed to be a white Gaussian processes with a standard deviation of $\sigma_\psi \approx 1$ μs [43]. To reduce measurement noise, pre-filters are applied to the observation data prior to the extended Kalman filter (cf. [33]).

Fig. 4 depicts the mobile trajectories obtained from three drive test scenarios: urban, suburban, and walking. The cell size is approximated by a 1 km $\times$ 1 km square and 100 initial samples are used as training data in all scenarios. The mobility state estimation procedure generates a sequence of mobility state estimates $\{\hat{\boldsymbol{s}}_2, \cdots, \hat{\boldsymbol{s}}_N\}$. Fig. 4 also shows, for each scenario, the estimated trajectory obtained using the AR-1 mobility estimator with TOA observations.

The sequence of position estimates $\{(\hat{x}_n, \hat{y}_n)\}$ can be compared quantitatively against the sequence of actual positions $\{(x_n, y_n)\}$ in terms of root mean squared error (RMSE) as a figure of merit, defined by

$$\text{RMSE} = \sqrt{\frac{1}{N-1}\sum_{n=2}^{N}[(\hat{x}_n - x_n)^2 + (\hat{y}_n - y_n)^2]}. \tag{29}$$

Fig. 5 shows the RMSE performance of mobility estimation schemes based on the AR-1 and Position-AR models for three data sets using RSSI and TOA measurements when different number of training samples are used to initialize model parameters. Each point in the graphs of Fig. 5 shows the average RMSE, i.e., μ_{RMSE}, over 50 experiments and the error bars represent $\pm\sigma_{\text{RMSE}}$ for each point. Line segments connecting the data points are only used for clarity of graphs and they do not represent anything. The cell size is approximated by a 1 km $\times$ 1 km square.

From the graphs of Fig. 5 we observe that more training samples result in better RMSE performance for the scenarios of our study. A training set which is an accurate representation of the trajectory would be an ideal choice for parameter initialization. However, we are choosing the first few samples of the trajectories which might not represent the whole trajectories accurately. This difference is evident in Fig. 5, where the mobility tracking results for the suburban trajectory are smoother than the rest of the data sets as it is mostly comprised of straight line segments with fewer bends. The urban data set was obtained from a downtown area with orthogonal streets

and walking scenarios is also comprised of more curved segments. In such scenarios, a larger training set is recommended.

We also note that the Position-AR model requires the estimation of fewer parameters than the AR-1 model and hence requires fewer training samples for proper initialization. Furthermore, the Position-AR model shows stable performance when the training set size is varied, in contrast to the AR-1 model, which performs poorly for small training sets. With a sufficient training set, the RMSE performance of AR-1 model can be better than Position-AR model as the transformation matrix A_1 in AR-1 model is allowed to adapt with perturbations in movement characteristics. With typical values of noise variance, the mobility tracking performance with TOA measurements was superior to that with RSSI measurements for all operating scenarios considered in this study.

Table II shows the performance of mobility tracking based on the AR-1 and Position-AR models when no training data is provided. In both models, the noise covariance matrices $\hat{Q}_1^{(0)}$ and $\hat{Q}_2^{(0)}$ are each initialized to the 6×6 identity matrix and the initial state vector estimate, $\hat{\boldsymbol{s}}_{1|0}$, is initialized to the zero vector. For the AR-1 model, the transformation matrix is initialized as follows using similar relationships as shown in (3):

$$\hat{A}_1^{(0)} = \begin{bmatrix} A_x & 0_{3\times 3} \\ 0_{3\times 3} & A_y \end{bmatrix} \tag{30}$$

where

$$A_x = A_y = \begin{bmatrix} 1 & T & T^2/2 \\ 0 & 1 & T \\ 0 & 0 & \alpha \end{bmatrix},$$

T is the sampling interval, and α is given an arbitrary value of 0.5. We have removed the first 50 estimated location points from RMSE calculations to focus on the steady-state behavior of the mobility estimators. From Table II one sees that even without training data, the mobility estimator based on the Position-AR model tracks the mobile user with reasonable accuracy. By contrast, the AR-1 based mobility estimator produces large errors, especially when RSSI observations are used.

The last factor considered in our study is cell size, to show the effect of observation data from distant base stations. Training data size is kept at 100 samples for all data sets and 2 filters are used in the pre-filtering step (cf. [33]) for this experiment. Fig. 6 shows the RMSE performance for different cell sizes. The x-axis in Fig. 6 shows the length of each side of the square cell. An increase in cell size generally reduces estimation accuracy. TOA-based mobility tracking outperforms RSSI-based tracking in all of our experiments. Also, Fig. 6 shows that tracking based on TOA measurements is more resilient than that based on RSSI when distances between the mobile user and the base stations increase.

The simulation results show that the mobility state estimator performed with reasonable accuracy under the three different mobility scenarios with appropriate selection of operating conditions. In general, a larger training set is preferable if available and the three largest signal measurements should be chosen among all available values. Training phase could also be used to bootstrap the operational settings of mobility estimation scheme, e.g., the number of pre-filters (cf. [33]), noise covariance value, etc.

D. Comparison with Other Mobility Models

The AR-1 and Position-AR models can accurately represent trajectories generated by other stochastic mobility models. Models such as the random waypoint model may be used for generating mobility patterns in simulation environments, but generally cannot be used to track mobility in real-time as it is not straightforward to estimate the model parameters for real scenarios. The linear system model of mobility discussed in [18] can be used to develop a mobility state estimator [33]. However, the parameters of the model cannot be estimated in an optimal way and the estimator performs well until the model parameters represent accurately the dynamic behavior of the mobile unit. We generated trajectories, containing more than 1000 data points, using the linear dynamic system model [18], [19] and the random waypoint model [4], [48]. We then used the proposed mobility estimation scheme to track the generated trajectories. In applying the mobility estimator, we assumed that training sets of 100 data points for linear

system's trajectory and 300 samples for random waypoint trajectory were available to initialize the AR-1 and Position-AR models. The cell size is set as 1000 m $\times$ 1000 m and two pre-filters are used prior to the extended Kalman filter (cf. [33]).

The parameters of the linear system model of mobility were set as follows (cf. [18], [19]): $\alpha = 1000$ s^{-1}, $T = 1$ s and $\sigma_1 = 1$ dB. The discrete command processes $u_x(t)$ and $u_y(t)$ are independent semi-Markov processes, each of which was assumed to take on five possible levels of acceleration comprising the set $\{-0.5, -0.25, 0, 0.25, 0.5\}$ in units of m/s^2. The initial probability vector $\boldsymbol{\pi}$ for the semi-Markov model (SMM) governing $u_x(t)$ and $u_y(t)$ was initialized to a uniform distribution. The elements of the transition probability matrix for the SMM were initialized to a common value of $1/5$. We assumed that the dwell times in each state were uniformly distributed with a common mean value of $2T$. The RSSI and TOA measurements were generated in a similar manner to that specified in the test scenarios.

The sample mean and standard deviation of RMSE statistics collected from 50 simulations are given in Table III. The result shows that the estimator based on the AR-1 and Position-AR models were able to estimate appropriate model parameters and accurately track the trajectory generated by the linear dynamic system model with both RSSI and TOA measurements.

We also generated trajectories using the random waypoint model and applied our proposed integrated mobility estimator. The trajectories were generated within an area of 2000 m $\times$ 2000 m, centered at the origin. The speed of the mobile unit was uniformly distributed in the interval $[0, 60]$ m/s^2 and the mean pause time was assumed to be 1 s. The random waypoint model tends to generate trajectories with sharp turns, which are quite different from realistic mobility patterns. Nevertheless, the mobility estimator was able to accurately track the trajectory as shown in Table III.

The standard deviation of the RMSE is higher for the linear system model, as shown in Table III, than for the random waypoint model because the mobility patterns generated by the random waypoint model largely consist of straight-line segments in which the mobile user moves at a constant speed (i.e., zero acceleration). The autoregressive model based estimators are able

to track the speed quite accurately along these straight-line path segments. Most of the error in the tracking occurs at the waypoints at which a random destination point and speed are chosen according to the random waypoint model. We also performed some experiments with the random waypoint mobility model using different speed distributions, such as a constant speed of 30 m/s and exponential distribution with a mean speed of 30 m/s. In both cases we observed similar location tracking performance as shown in Table III. The estimation performance does not seemed to be affected by the speed distributions chosen for the random waypoint model.

VI. Conclusion

We proposed a mobility tracking scheme based on two autoregressive models of mobility, which we refer to as the *AR-1* and *Position-AR* models. The AR-1 and Position-AR models are relatively simple, yet provide more accurate representation of realistic mobility patterns than existing mobility models. Both models were validated using mobile trajectory data obtained from a cellular network, as well as simulated data obtained from the random waypoint and linear system models of mobility. The proposed mobility tracking scheme consists of an integrated scheme of MMSE (Minimum Mean Squared Error) parameter estimation and mobility state estimation based on Kalman filtering using observations of RSSI and TOA from the network. The scheme provides a viable solution to the two important issues of realistic mobility modeling and real-time mobility tracking for wireless networks.

We have also analyzed the effects of different operational settings on the performance of mobility estimation scheme using both models and both observations. The Position-AR model requires a smaller number of training samples for initialization than the AR-1 model and is more resilient to perturbations in operating conditions. With typical values of noise variance for both types of observation data, mobility tracking performance using TOA (Time-of-Arrival) measurements was superior to the performance using RSSI (Received Signal Strength Indication) measurements in our experiments.

The proposed mobility tracking schemes can enable mobility-aware applications, which can improve performance or provide new services in wireless networks. In cellular networks, for

example, the mobility estimation scheme could be used to predict cell crossings for smoother handoffs and more efficient resource allocation [18]. The mobility tracking scheme could also be adapted for mobile ad hoc networks (cf. [49]).

ACKNOWLEDGEMENTS

We wish to acknowledge Mohammed Benchaaboune for providing the drive test data used to validate the mobility models and Dr. Asad Zaman of Lahore University of Management Sciences (LUMS), Pakistan, for his useful feedback.

APPENDIX

The matrix H_n in equation (22) is given by

$$H_n = (\boldsymbol{h}'_{n,1}, \cdots \boldsymbol{h}'_{n,m})', \tag{31}$$

where $\boldsymbol{h}_{n,i}$ is the ith row of H_n for $i = 1, 2, 3$.

1) For RSSI:

$$\boldsymbol{h}_{n,i} = \frac{-10\gamma}{(d_{n,i})^2}(x_n - a_i, 0, 0, y_n - b_i, 0, 0) \tag{32}$$

where $i = 1, 2, 3$.

2) For TOA:

$$\boldsymbol{h}_{n,i} = \frac{1}{c(d_{n,i})}(x_n - a_i, 0, 0, y_n - b_i, 0, 0) \tag{33}$$

where $i = 1, 2, 3$.

REFERENCES

[1] C. Bettstetter, "Smooth is better than sharp: A random mobility model for simulation of wireless networks," in *Proc. of ACM MSWiM*, pp. 19–27, July 2001.
[2] T. Camp, J. Boleng, and V. Davies, "Survey of mobility models for ad hoc network research," *Wireless Communication and Mobile Computing (WCMC), Special issue on Mobile Ad Hoc Networking*, vol. 2, no. 5, pp. 483–502, 2002.
[3] I. F. Akyildiz, Y. B. Lin, W. R. Lai, and R. J. Chen, "A new random walk model for PCS networks," *IEEE Journal of Selected Areas in Communications*, vol. 18, no. 7, pp. 1254–1260, 2000.
[4] D. Johnson and D. Maltz, "Dynamic source routing in ad hoc wireless networks," *Mobile Computing*, vol. 353, 1996.
[5] H. Stark and J. W. Woods, *Probability and Random Processes with Applications to Signal Processing*. Englewood Cliffs, NJ: Prentice Hall, 3rd ed., 2001.
[6] B. Liang and Z. J. Haas, "Predictive distance-based mobility management for multidimensional PCS networks," *IEEE/ACM Trans. on Networking*, vol. 11, no. 5, pp. 718–732, 2003.
[7] H. Kobayashi, S. Z. Yu, and B. L. Mark, "An integrated mobility and traffic model for resource allocation in wireless networks," in *Proc. 3rd ACM Int. Workshop on Wireless Mobile Multimedia*, (Boston), pp. 39–47, Aug. 2000.
[8] J. Yoon, M. Liu, and B. Noble, "Random waypoint considered harmful," in *Proc. IEEE INFOCOM*, vol. 2, pp. 1312–1321, March 2003.
[9] J. Yoon, M. Liu, and B. Noble, "Sound mobility models," in *Proc. ACM MOBICOM*, pp. 205–216, September 2003.

[10] A. Jardosh, E. M. Belding-Royer, K. Almeroth, and S. Suri, "Towards realistic mobility models for mobile ad hoc networks," in *Proc. of ACM MOBICOM '03*, pp. 217–229, September 2003.

[11] J. Härri and F. Filali and C. Bonnet, "A framework for mobility models generation and its application to inter-vehicular networks," in *Proc. of IEEE Wireless Networks, Communications and Mobile Computing 2005*, vol. 1, pp. 42–47, June 2005.

[12] P. A. Dintchev, B. Perez-Quiles, and E. Bonek, "An improved mobility model for 2G and 3G cellular systems," in *Proc. of IEEE 3G Mobile Communication Technologies 2004*, vol. 1, pp. 402–406, 2004.

[13] A. Momen, A. Mirzaee, and S. Masajedian, "An analytical random direction-based method in user mobility modeling for wireless networks," in *Proc. IEEE PIMRC '05*, vol. 3, pp. 2050– 2057, Sept. 2005.

[14] G. Lu and G. M. D. Belis, "Study on environment mobility models for mobile ad hoc network: hotspot mobility model and route mobility model," in *Proc. IEEE Wireless Networks, Communications and Mobile Computing Conf.*, vol. 1, pp. 808–813, June 2005.

[15] S. Bittner, W. U. Raffel, and M. Scholz, "The area graph-based mobility model and its impact on data dissemination," in *Proc. of IEEE PerComm '05*, vol. 1, pp. 268–272, March 2005.

[16] A. K. H. Souley and S. Cherkaoui, "Advanced mobility models for ad hoc network simulations," in *Proc. of IEEE ICW '05*, vol. 1, pp. 50–55, August 2005.

[17] F. Legendre, V. Borrel, M. D. D. Amorim, and S. Fdida, "Reconsidering microscopic mobility modeling for self-organizing networks," *IEEE Network*, vol. 20, pp. 4–12, Nov-Dec 2006.

[18] T. Liu, P. Bahl, and I. Chlamtac, "Mobility modeling, location tracking, and trajectory prediction in wireless ATM networks," *IEEE J. Selected Areas in Comm.*, vol. 16, pp. 922–936, August 1998.

[19] B. L. Mark and Z. R. Zaidi, "Robust mobility tracking for cellular networks," in *Proc. IEEE ICC*, vol. 1, pp. 445–449, May 2002.

[20] M. Hellebrandt and R. Mathar, "Location tracking of mobiles in cellular radio networks," *IEEE Trans. on Vehicular Technology*, vol. 48, pp. 1558–1562, Sept. 1999.

[21] Z. Yang and X. Wang, "Joint mobility tracking and hard handoff in cellular networks via sequential Monte Carlo filtering," in *Proc. IEEE INFOCOM*, vol. 2, pp. 968–975, June 2002.

[22] L. Mihaylova, D. Angelova, S. Honary, D. R. Bull, C. N. Canagarajah, and B. Ristic, "Mobility tracking in cellular networks using particle filtering," *IEEE Trans. Wireless Communications*, vol. 6, pp. 3589 – 3599, October 2007.

[23] Z. R. Zaidi and B. L. Mark, "Mobility estimation for wireless networks based on an autoregressive model," in *Proc. IEEE Globecom*, vol. 6, pp. 3405–3409, Nov.-Dec. 2004.

[24] R. G. Brown and P. Y. Hwang, *Introduction to Random Signals and Applied Kalman Filtering*. New York: John Wiley & Sons, 3rd ed., 1997.

[25] J. S. Lim and A. V. Oppenheim, *Advanced Topics in Signal Processing*. Englewood Cliffs, NJ 07632: Prentice Hall, 1987.

[26] J. Kempf, J. Wood, and G. Fu, "Fast mobile IPv6 handover packet loss performance," in *Proc. IEEE Wireless Networking and Communications Conference (WCNC)*, (New Orleans, LA), March 2003.

[27] Y. Gwon, G. Fu, and R. Jain, "Fast Handoffs in Wireless LAN Networks Using Mobile Initiated Tunneling Handoff Protocol for IPv4 (MITHv4)," in *Proc. of IEEE WCNC 2003*, (New Orleans), pp. 1248–1252, March 2003.

[28] Z. R. Zaidi and B. L. Mark, "A mobility-aware handoff trigger scheme for seamless connectivity in cellular networks," in *Proc. IEEE VTC Fall*, vol. 5, pp. 3471–3475, Sept. 2004.

[29] X. Hong, M. Gerla, G. Pei, and C. C. Chiang, "A group mobility model for ad hoc wireless networks," in *Proc. of ACM MSWiM*, pp. 53–60, August 1999.

[30] D. Lam, D. C. Cox, and J. Widom, "Teletraffic modeling for personal communication services," *IEEE Commun. Magazine*, vol. 35, pp. 79–87, October 1997.

[31] T. Tugcu and C. Ersoy, "Application of a realistic mobility model to call admission in DS-CDMA cellular systems," in *Proc. IEEE VTC*, pp. 1047–1051, 2001.

[32] J. Scourias and T. Kunz, "An activity-based mobility model and location management simulation frameworks," in *Proc. ACM MSWiM*, pp. 61–68, Aug. 1999.

[33] Z. R. Zaidi and B. L. Mark, "Real-time Mobility Tracking Algorithms for Cellular Networks based on Kalman Filtering," *IEEE Trans. on Mobile Computing*, vol. 4, pp. 195–208, March-April 2005.

[34] J. J. Caffery Jr., *Wireless Location in CDMA Cellular Radio Systems*. Norwell, Massachusetts: Kluwer Academic Publishers, 1999.

[35] P. Deng and P. Z. Fan, "An AOA assisted TOA positioning system," in *Proc. of WCC-ICCT '00*, vol. 2, pp. 1501–1504, 2000.

[36] L. Cong and W. Zhuang, "Hybrid TDOA/AOA mobile user location for wideband CDMA cellular systems," *IEEE Trans. on Wireless Communications*, vol. 1, pp. 1439–1447, July 2002.

[37] Y. Jeong, H. You, W. C. Lee, D. Hong, D. H. Youn, and C. Lee, "A wireless position location system using forward pilot signal," in *Proc. of IEEE VTC '00*, pp. 1354–1357, 2000.

[38] A. Abrardo, G. Benelli, C. Maraffon, and A. Toccafondi, "Performance of TDOA-based radiolocation techniques in CDMA urban environments," in *Proc. of IEEE ICC '02*, pp. 431–435, May 2002.

[39] G. Yost and S. Panchapakesan, "Automatic location identification using a hybrid technique," in *Proc. IEEE VTC*, pp. 264–267, 1998.

[40] M. Gudmundson, "Correlation model for shadowing fading in mobile radio systems," *Electronic Letters*, vol. 27, pp. 2145–2146, November 1991.

[41] G. L. Stüber, *Principles of Mobile Communication*. Massachusetts: Kluwer Academic Publishers, 2nd ed., 2001.

[42] D. Hong and S. S. Rappaport, "Traffic model and performance analysis for cellular mobile radio telephone systems with prioritized and nonprioritized handoff procedures," *IEEE Trans. on Vehicular Technology*, vol. 35, pp. 77–91, August 1986.

[43] H. C. So and E. M. K. Shiu, "Performance of TOA-AOA hybrid mobile location," *IEICE Trans. on Fundamentals*, vol. E86-A, pp. 2136–2138, August 2003.

[44] A. P. Dempster, N. M. Laird, and D. B. Rubin, "Maximum likelihood from incomplete data via the EM algorithm," *Journal of Royal Statistical Society, Series B (Methodological)*, vol. 39, no. 1, pp. 1–38, 1977.

[45] C. F. J. Wu, "On the Convergence Properties of the EM Algorithm," *The Annals of Statistics*, vol. 11, no. 1, pp. 95–103, 1983.

[46] W. Mendenhall and T. Sincich, *Statistics for the Engineering and Computer Sciences*. San Francisco, CA: Dellen Publishing Co., Macmillan Inc., 1988.

[47] R. A. Johnson and D. W. Wichern, *Applied Multivariate Statistical Analysis*. Upper Saddle River, New Jersey: Prentice Hall, 2002.

[48] J. Broch, D. A. Maltz, D. B. Johnson, Y. C. Hu, and J. Jetcheva, "A performance comparison of multi-hop wireless ad hoc network routing protocols," in *Proc. of ACM Mobicom*, pp. 85–97, October 1998.

[49] Z. R. Zaidi and B. L. Mark, "A mobility tracking model for wireless ad hoc networks," in *Proc. IEEE WCNC '03*, vol. 3, pp. 1790–1795, March 2003.

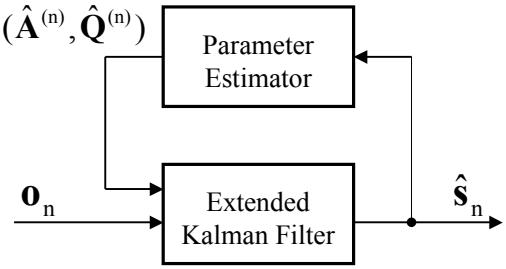

Fig. 1. Mobility tracking via an integrated mobility state and parameter estimator.

TABLE I
R^2 VALUES FOR SAMPLE DATA SETS.

Data sets	Training samples	R^2 AR-1	R^2 Position-AR
suburban (driving)	100	0.99	1.0
urban (driving)	500	0.95	1.0
GMU (walking)	100	0.94	0.99

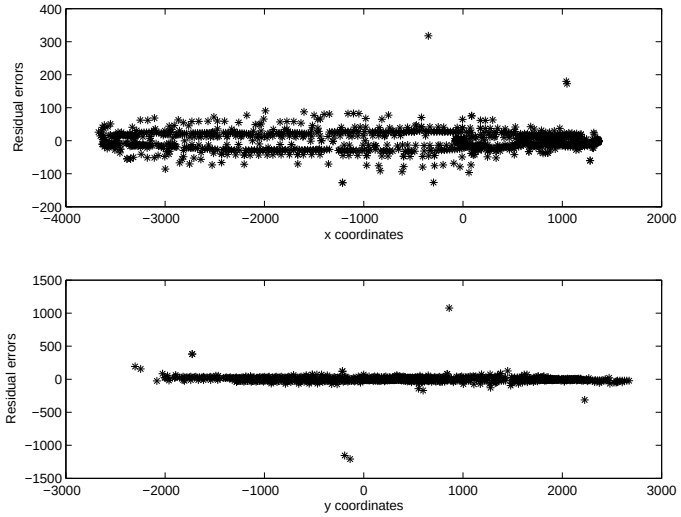

Fig. 2. Independence of residual error for the Position-AR model.

TABLE II
RMSE OF ESTIMATION ALGORITHMS WHEN NO TRAINING DATA IS AVAILABLE.

	RSSI		TOA	
Scenarios	AR-1 (μ_{RMSE}, σ_{RMSE}) (m)	Position-AR (μ_{RMSE}, σ_{RMSE}) (m)	AR-1 (μ_{RMSE}, σ_{RMSE}) (m)	Position-AR (μ_{RMSE}, σ_{RMSE}) (m)
Urban	(5243.1, 143.1)	(48.28, 2.45)	(612.6, 1310.8)	(23.08, 0.54)
Suburban	(2246.4, 5.4)	(55.16, 2.7)	(22.5, 3.14)	(32.97, 1.02)
GMU walking	(373.48, 0)	(51.26, 2.3)	(373.04, 3.1)	(38.43, 1.2)

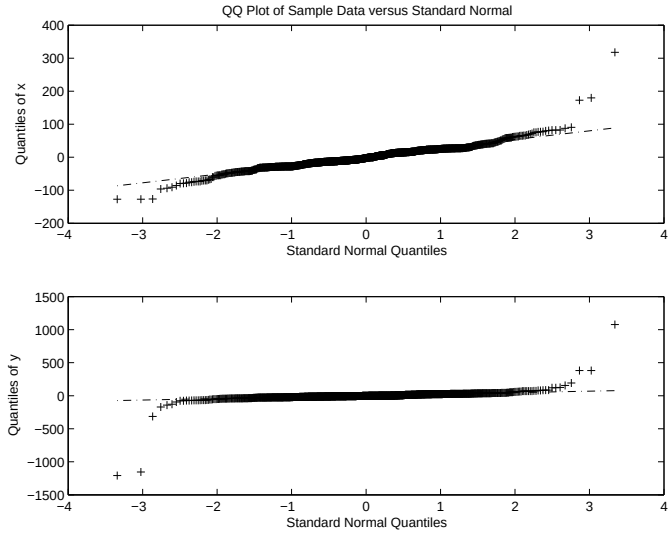

Fig. 3. Q-Q plots for residual error in the Position-AR model.

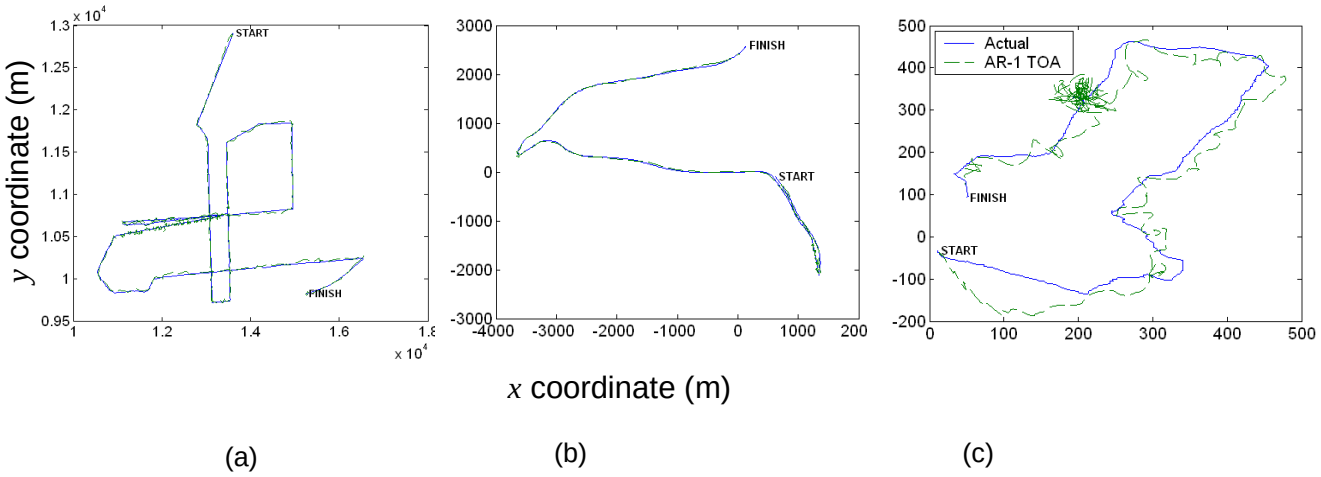

Fig. 4. Actual and estimated trajectories using AR-1 model and TOA observations in (a) urban, (b) suburban, and (c) GMU walking scenarios.

TABLE III
RMSE OF ESTIMATION ALGORITHM - STOCHASTIC MODELS.

	RSSI		TOA	
Models	AR-1 (μ_{RMSE}, σ_{RMSE}) (m)	Position-AR (μ_{RMSE}, σ_{RMSE}) (m)	AR-1 (μ_{RMSE}, σ_{RMSE}) (m)	Position-AR (μ_{RMSE}, σ_{RMSE}) (m)
Linear system	(68.93, 8.57)	(52.46, 6.8)	(43.29, 4.33)	(38.14, 3.56)
Random waypoint	(49.69, 3)	(52.97, 4.8)	(21.44, 1.2)	(26.28, 1.4)

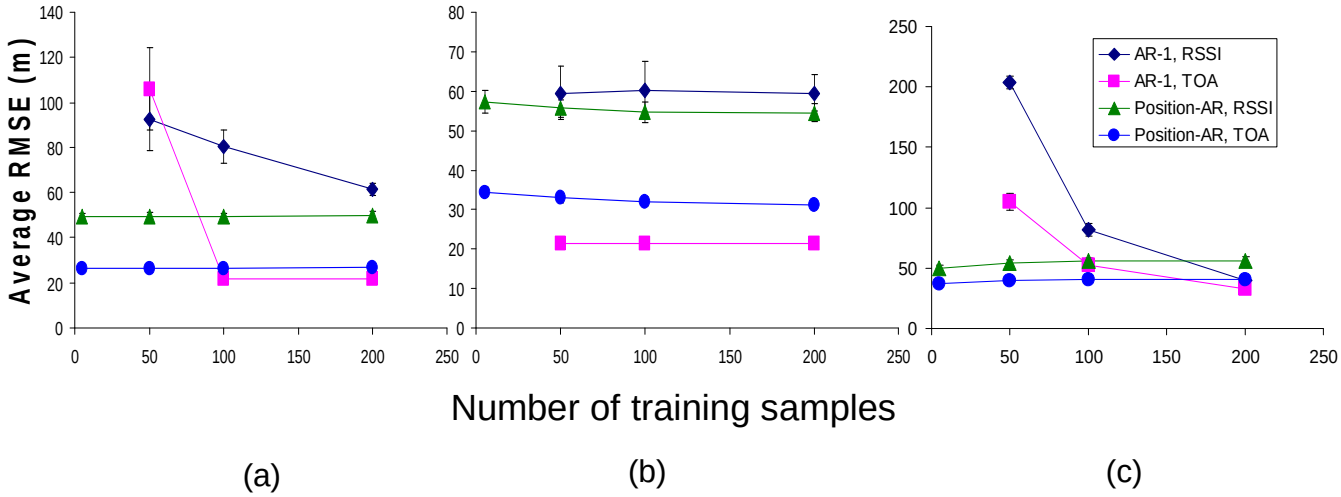

Fig. 5. RMSE performance vs. number of training samples for (a) urban, (b) suburban, and (c) GMU walking scenarios.

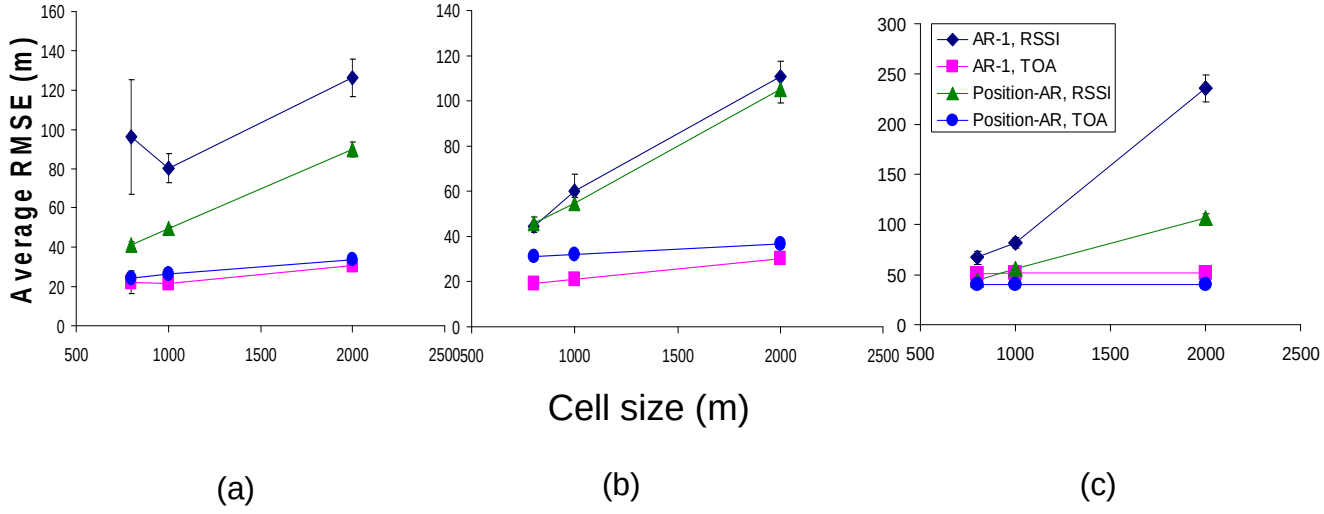

Fig. 6. RMSE performance vs. cell size for (a) urban, (b) suburban, and (c) GMU walking scenarios.